A&A 516, A50 (2010)
DOI: 10.1051/0004-6361/200913624

Astronomy & Astrophysics

Coronal hole boundaries evolution at small scales

II. XRT view. Can small-scale outflows at CHBs be a source of the slow solar wind?⋆

S. Subramanian, M. S. Madjarska, and J. G. Doyle

Armagh Observatory, College Hill, Armagh BT61 9DG, N. Ireland
e-mail: madj@arm.ac.uk

Received 8 November 2009 / Accepted 12 April 2010

ABSTRACT

Aims. We aim to further explore the small-scale evolution of coronal hole boundaries using X-ray high-resolution and high-cadence images. We intend to determine the fine structure and dynamics of the events causing changes of coronal hole boundaries and to explore the possibility that these events are the source of the slow solar wind.
Methods. We developed an automated procedure for the identification of transient brightenings in images from the X-ray telescope on-board Hinode taken with an Al Poly filter in the equatorial coronal holes, polar coronal holes, and the quiet Sun with and without transient coronal holes.
Results. We found that in comparison to the quiet Sun, the boundaries of coronal holes are abundant with brightening events including areas inside the coronal holes where closed magnetic field structures are present. The visual analysis of these brightenings revealed that around 70% of them in equatorial, polar and transient coronal holes and their boundaries show expanding loop structures and/or collimated outflows. In the quiet Sun only 30% of the brightenings show flows with most of them appearing to be contained in the solar corona by closed magnetic field lines. This strongly suggests that magnetic reconnection of co-spatial open and closed magnetic field lines creates the necessary conditions for plasma outflows to large distances. The ejected plasma always originates from pre-existing or newly emerging (at X-ray temperatures) bright points.
Conclusions. The present study confirms our findings that the evolution of loop structures known as coronal bright points is associated with the small-scale changes of coronal hole boundaries. The loop structures show an expansion and eruption with the trapped plasma consequently escaping along the "quasi" open magnetic field lines. These ejections appear to be triggered by magnetic reconnection, e.g. the so-called interchange reconnection between the closed magnetic field lines (BPs) and the open magnetic field lines of the coronal holes. We suggest that these plasma outflows are possibly one of the sources of the slow solar wind.

Key words. Sun: atmosphere – Sun: corona – methods: observational – methods: data analysis

1. Introduction

Coronal holes (CHs) are regions of predominantly unipolar coronal magnetic fields with a significant component of the magnetic field open into the heliosphere. They are visible in spectral lines emitting at coronal temperatures as dark areas when compared to the quiet Sun, while in the chromospheric He I 10830 Å line they appear bright. For detailed introduction on coronal holes see Madjarska & Wiegelmann (2009, hereafter Paper I). CHs are identified as the source of the fast solar wind with velocities of up to ≈800 km s^{-1} (Krieger et al. 1973). In contrast, the slow wind has velocities around 400 km s^{-1} and is more dense, and variable in nature when compared to the fast solar wind. von Steiger (1996) found from Ulysses satellite data that the elemental composition of the fast wind is similar to the elemental composition of the photosphere. The slow solar wind is enriched with low first ionization potential (FIP) elements by a factor of 3–5 greater than in the photosphere (with respect to hydrogen) while higher FIP elements were found at solar surface abundances. The FIP effect describes the element abundance anomalies (the enhancement of elements with low FIP such as Fe, Mg and Si over those with high FIP like Ne and Ar) in the upper solar atmosphere and solar wind, and can give a clue on the origin of both the fast and the slow solar winds. von Steiger (1996) concluded that the fast and slow solar winds not only differ in their kinetics but also in their composition of elements.

Woo et al. (2004) suggested that the release of trapped plasma in closed loop structures by magnetic reconnection could play a significant role in the solar wind flow. Such reconnection between the open and closed magnetic field lines presumably happens continuously at coronal hole boundaries. Wang et al. (1998) investigated the ejection of plasma blobs from the streamer belt linked to the slow wind and concluded that magnetic reconnection between the distended streamer loops and the open magnetic field lines might be behind the plasma ejection. They also suggested that this ejection cannot account for all the slow solar wind and a major component should, therefore, originate outside the helmet streamers, i.e. from inside the coronal holes. Madjarska et al. (2004) found non-Gaussian profiles along the boundaries of an equatorial extension of a polar CH in the mid- and high-transition region lines N IV 765 Å and Ne VIII 770 Å, respectively, recorded with the Solar Measurement of Emitted Radiation (SUMER) spectrometer on-board the Solar and Heliospheric Observatory (SoHO). The authors suggested that these profiles are the signature of magnetic reconnection occurring between the closed magnetic

⋆ 4 movies are only available in electronic form at http://www.aanda.org

Table 1. Description of the XRT data used in the present study.

Date	Remark	Observing period of time (UT)	Field-of-view (arcsec)	Exposure time (s)
09/11/07	ECH	06:35–14:59	366 × 366	16
12/11/07	ECH	01:17–10:59	374 × 374	16
14/11/07	ECH	00:12–11:11	374 × 374	16
16/11/07	ECH	18:07–23:58	370 × 370	16
16/12/08	PCH	10:02–17:52	362 × 337	23
20/09/07	PCH	12:22–18:05	1018 × 291	16
10/01/09	QS	11:30–17:27	370 × 370	23
13/01/09	QS	11:22–17:41	370 × 370	23
29/11/07	QS with TCH	18:17–23:59	506 × 506	23

Notes. ECH − equatorial coronal hole, PCH − polar coronal hole, TCH − transient coronal hole.

field lines of the quiet Sun and the open of the coronal hole. Similar activity was reported by Doyle et al. (2006) along the boundary of a polar CH.

In Paper I we demonstrated that although isolated equatorial CH and equatorial extension of polar CH maintain their general shape during several solar rotations, a closer look at their day-by-day and even hour-by-hour evolution demonstrates significant dynamics. We showed that small-scale loops which are abundant along coronal hole boundaries contribute to the small-scale evolution of coronal holes. We suggested that these dynamics are triggered by continuous magnetic reconnection already proposed by Madjarska et al. (2004). The next step of our research was to analyse images taken with the X-ray Telescope (XRT) on-board Hinode.

Seen in XRT images, CHs are highly structured and dynamic at small scales. High cadence XRT data reveal in great detail the fine structure of coronal bright points (BPs) and X-ray jets associated with them. X-ray jets are collimated transient ejection of coronal plasma, first reported with the Solar X-ray telescope (SXT) onboard Yohkoh (Shibata et al. 1992). They are believed to result from magnetic reconnection (Shibata et al. 1994) and represent plasma outflows from the reconnection site. Recently, Moreno-Insertis et al. (2008) presented three-dimensional simulations of flux emergence in CH combined with spectroscopic and imager observations from XRT and EIS/Hinode of an X-ray jet. The authors report that a jet resulting from magnetic reconnection is expelled upward along the open reconnected field lines with values of temperature, density, and velocity in agreement with the XRT and EIS observations. Shimojo et al. (1996) reported 100 jets over 6 months in SXT images from the Yohkoh while Savcheva et al. (2007) upgraded this number to an average of 60 jet events per day in polar coronal holes. The authors concluded that jets preferably occur inside polar coronal holes (PCH).

We should note that although TRACE images which have higher spatial resolution were used in Paper I, the detailed structure of the dynamic changes along CH boundaries was hard to distinguish. A reason for that is the effect of stray light in the TRACE extreme-ultraviolet (EUV) telescope reported recently by DeForest et al. (2009). The authors found that 43% of the light which enters TRACE through the Fe IX/X 171 Å filter is scattered either through diffraction off the entrance filter grid or through other non-specific effects. This creates a haze effect and especially effects the visibility of small-scale bright structures.

Other transient structures seen in coronal holes are the so-called plumes observed off-limb above the North and South polar coronal holes. They were first observed in white light as ray like structures (Saito 1965). They are also observed at EUV and soft X-ray temperature (Ahmad & Webb 1978) as coronal outflow structures similar to coronal jets, but hazy in nature with no sharp boundaries unlike jets. They represent denser and cooler outflows with respect to the surrounding media and are observed to extend from coronal BPs. They can extend up to 30 $R_{\odot}$ from the solar disk center in a plane image (DeForest et al. 2001) and are observed to be in a steady state for at least 24 h (Deforest et al. 1997). The X-ray jets have been identified as precursors for the plume formation (Raouafi et al. 2008). Recently, Wang & Muglach (2008) identified coronal plumes inside equatorial coronal holes. They found that the plumes are analogous to polar coronal plumes. On the disk they are seen as a diffuse structure with a bright core and associated with EUV BPs.

The present study is a continuation of Paper I and presents results from the analysis of high-cadence/high-resolution images of coronal holes (equatorial, polar and transient) and quiet Sun from XRT/Hinode. We aim to establish which type of event generates the non-Gaussian profiles registered at CH boundaries by Madjarska et al. (2004) and how they are related to the small-scale BPs evolution along coronal hole boundaries as reported in Paper I. In Sect. 2 we describe the data used for our study. Section 3 outlines an automatic brightening identification procedure. In Sect. 4, we give the obtained results and draw some conclusions on the outcome of our study. Finally, in Sect. 5 we discuss the implication of our result to the understanding of the nature of coronal hole boundaries evolution at small scale and the possible contribution of these events to the formation of the slow solar wind.

2. Data, reduction and preparation

We used images from the X-ray Telescope (Golub et al. 2007) on-board Hinode taken during a dedicated observing run of an isolated equatorial coronal hole (ECH), a Southern polar coronal hole and quiet Sun regions. The ECH was tracked from the West to the East limb from 8 to 10 h per day for 4 days. The Southern polar CH was observed for one day while the quiet Sun regions over 2 days. All data were taken with an Al Poly filter which has a well pronounced temperature response at $\log T_{\max} \approx 6.9$ K. XRT images have an angular pixel size of $1'' \times 1''$ at full resolution. They were recorded with 16 s and 23 s exposure time and a cadence of about 40 s. We also used randomly selected quiet Sun data with transient coronal holes (TCHs) and a Northern polar coronal hole observation. Further details on the data can be found in Table 1.

The data were reduced using the standard procedures, which include flat-field subtraction, dark current removal, despiking, normalisation to data number per second to account for the

variations in exposure time, satellite jitter and orbital variation corrections. The images were then de-rotated to a reference time to compensate for the solar rotation. A common field-of-view (FOV) was selected from all the images for each day. We then prepared an array with dimensions (nx, ny, nf), where nx is the number of Solar_X pixels, ny is the number of Solar_Y pixels and nf is the number of images. Each image was binned to 4×4 pixels^2 in order to improve the signal-to-noise ratio and reduce the data points (and subsequently the computational time). The binned images were used to produce light curves of nf points for each pixel. These light curves were the input for an identification procedure which will be discussed in the next section.

3. Brightening identification procedure

We developed an automatic identification procedure to distinguish small-scale intensity enhancements in XRT images. While the visual identification of large events such as jets from bright points give good results, it is difficult to identify and track small-scale events, especially on the quiet Sun high background emission or over pre-existing bright coronal loop structures (e.g. bright points, active regions etc.). We eliminated all light curves which show no activity or minimum activity comparable to the noise level.

The first step of the identification procedure was to define the background emission for each light curve. The light curves were smoothed over a window of 5 frames to remove the spikiness in the background. Due to a difference in the background emission between the quiet Sun and the CHs, it was necessary to set two different thresholds for further analysis. The thresholds we used were 1.8 times the mean emission value for the CHs and 1.3 times the mean emissivity for the QS. The comparatively higher threshold set for the CH light curves helped to eliminate the high fluctuations of the low emission background. Light curves with a maximum value less than these thresholds were neglected. Any point in the light curve was considered as a peak if its value was greater than the threshold and also greater than the average of the two preceding points, and the average of two successive points. All the values below the threshold were considered as local minima. Each identified peak was traced back on either side to identify the minimum from the local minima. The value of all the points between the two identified minima for each peak were set to zero in the light curve and thereby from the average over the rest of the light curve ($I_{\rm av}$), we computed the standard deviation (SD). The new background (BG) was obtained as BG = $I_{\rm av}$ + 1.1 × SD.

The next step was the actual identification of intensity enhancements. A new threshold of 2 × BG for CHs and 1.3 × BG for QS was set using the above calculated background. Intensity increases above these thresholds with corresponding minima less than BG and duration less than 45 min were identified. A pixel brightening was considered only if all the above mentioned conditions were satisfied. The threshold was calculated with a trial and error method.

The peaks having a duration of more than 45 min were examined separately. The closest local minimum on either side of the peak were traced back. If the difference between the peak and the minimum were greater than the BG for the CHs and 0.3 × BG for the QS with the duration less than 45 min, then they were considered. Also the peaks which have one minimum that was either in the beginning or at the end of the light-curve were evaluated with the same criteria, in order not to miss any real event. Any intensity enhancements in the coronal holes, the quiet Sun or over pre-existing bright loop structures which satisfy the above criteria could be identified by our procedure.

4. Results and discussion

As it has been described in Sect. 2, we made a selection of data which comprised observations of different features on the Sun: equatorial and polar coronal holes as well as quiet Sun regions with and without transient coronal holes. In Figs. 1–4 we display examples of an X-ray image from each different region. Our intention was to find out whether the changes we have seen so far along CHBs (Madjarska et al. 2004; and Paper I) are unique for CH regions, i.e. regions of open magnetic field lines. These data also permit to resolve the fine structure of individual features and follow their dynamics at high cadence. To each dataset we applied the identification procedure described above. This procedure provided us with the following information: (i) light curves which contain one or more radiance enhancement identified as brightenings following the criteria given in Sect. 3; (ii) the start and end time of each radiance enhancement; (iii) the brightening positions in pixel numbers. As we produced light curves by binning over 4 × 4 pixels^2, imprints of brightening events with spatial scales larger than 4 × 4 pixels^2 were observed in more than one light curve. This made visual grouping of identified bright pixels essential to distinguish each event. Grouping of the features into individual events was done by playing the image sequence of each dataset with the identified brightenings over-plotted at corresponding times (see the online movies). Clusters of bright pixels identified next to each other with similar lightcurves were grouped into events. The events showing plasma outflows (i.e. plasma moving along quasi-straight trajectories) were classified as jets, while events exhibiting plasma blobs moving along curved trajectories or just brightening increase in a group of pixels were classified as unresolved brightenings events. The so-called space-time plot was also used to investigate the plasma motion in the form of a jet and to determine their proper motion. A space-time plot was produced by averaging over a slice of 3 pixels wide and 100 pixels long from each image, cut along the jet, i.e. in the direction of plasma propagation and then plotting that in time (Shimojo et al. 2007; and Subramianian, Ph.D. thesis 2010). We were able to group more than 95% of the identified bright pixels. The ungrouped pixels (≤5%) comprise bright pixels identified at the edges of images and above bad pixels. The pixels identified in the beginning of each dataset which could not be classified due to the lack of coverage of the whole event and the pixels identified with a time lapse over their lifetimes were also rejected from counting.

The visual grouping of identified bright pixels into events can be found in Table 2. We defined a coronal hole boundary region (CHBR) as the region ±15″ on both sides of the contour line defining the CH boundary. Additionally, animated image sequences with over-plotted identified brightenings at corresponding times are available online (cf. Fig. 1).

The first and the most important result of this study is easily noticeable from Figs. 1–4 the boundaries of coronal holes are abundant with brightening events which appear much larger than the same phenomena in the quiet-Sun region. We separated the events visually into two groups, events with plasma outflows or jet-like events and events without outflows or simple brightenings. The equatorial coronal hole data, observed near the disk center, show twice as many jet-like and simple brightening events in the CHBRs (as defined above) as compared to the CH regions. In contrast, polar coronal hole data and ECH close to the West limb (2007 November 16) show a higher number of

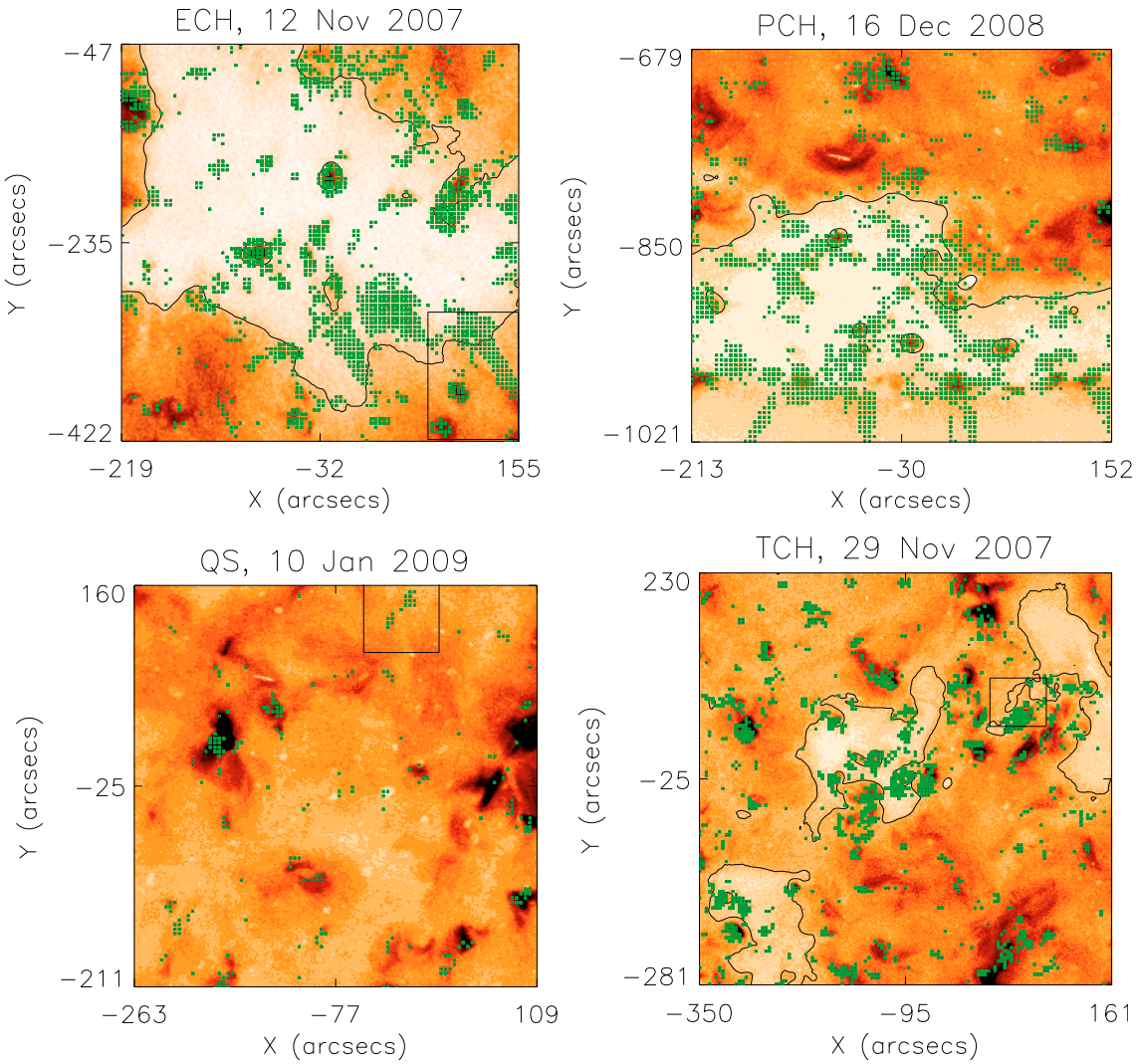

Fig. 1. Equatorial coronal hole (*top left*), polar CH (*top right*), quiet Sun (*bottom left*) and quiet Sun with TCHs (*bottom right*) with the positions of all the corresponding identified brightening pixels over-plotted. The CH boundaries are outlined with a black line. The over-drawn rectangles correspond to the field-of-views shown in Figs. 5–7. Time sequences can be found in movies online.

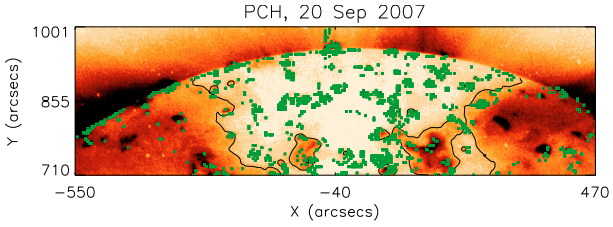

Fig. 2. Polar coronal hole observed by XRT on 2007 September 20 with the positions of all the identified brightening pixels over-plotted.

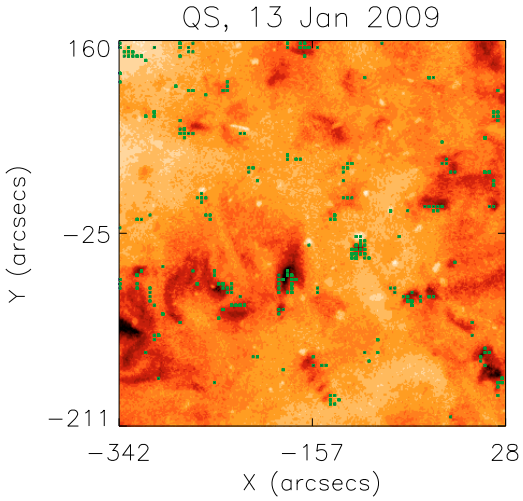

Fig. 3. Quiet Sun observed by XRT on 2009 January 13 with the positions of all the identified brightening pixels over-plotted.

events inside the CH as well as in the CHBRs suggesting that this can be due to the line-of-sight effect. However, further investigation is needed on a larger number of datasets.

If we assume that the magnetic reconnection responsible for the occurrence of jet-like events takes place predominantly between closed and open magnetic field lines, then the number of reconnection events producing outflows will be always higher in the CH boundary region since open and closed magnetic field lines are continuously pushed together by different processes such as convection, differential rotation, meridian motions etc. Inside coronal holes, where the number of bipolar systems and the corresponding closed loop structures are limited, the number of jet-like events will therefore be lower. For the transient

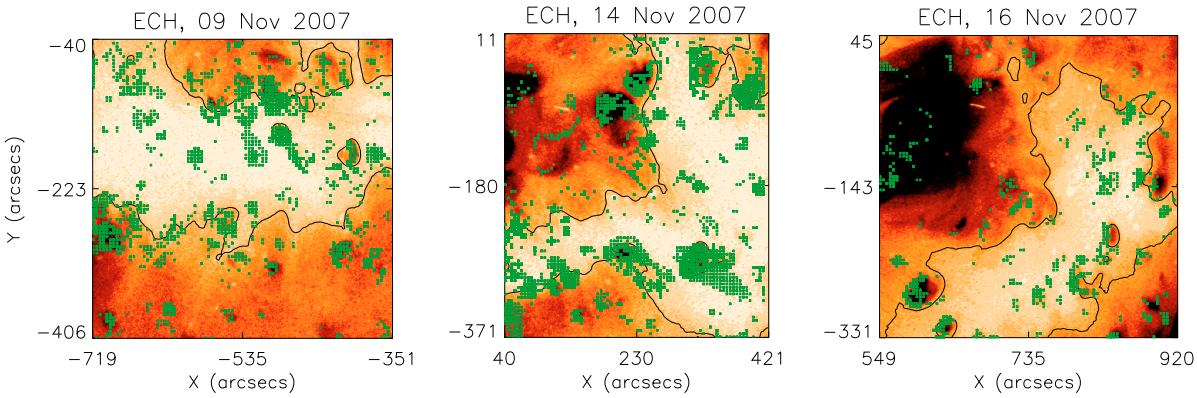

Fig. 4. Equatorial coronal hole observed by XRT on 2007 November 9, 14 and 16 with the positions of all the identified brightening pixels over-plotted. The CH boundaries are over-plotted with a black solid line.

Table 2. Number of events over 24 h per 100 × 100 arcsec^2 identified inside the coronal holes (CH), in coronal hole boundary regions (CHBR) and in the quiet Sun (QS).

Date	No of events identified with plasma outflows			No of unresolved events identified with no plasma outflows		
	CH	CHBR	QS	CH	CHBR	QS
09/11/07	29	40	6	6	26	8
12/11/07	16	57	6	2	17	7
14/11/07	10	51	1	16	41	7
16/11/07	56	32	–	44	33	12
16/12/08	99	86	6	31	14	33
20/09/07	57	72	4	5	7	9
10/01/09	–	–	6	–	–	17
13/01/09	–	–	9	–	–	14
29/11/07	–	64	7	–	62	14

coronal hole regions, the separation of the coronal hole boundaries region (30″ wide) from the coronal holes, for estimating the number of events in each region, is more difficult due to the very small size of these coronal holes. Therefore, here we consider that these CHs represent entirely a boundary region. The number of events found in these TCHs is several times larger than in the quiet Sun (both with and without outflows).

The plasma ejected during the outflow events always originates from pre-existing or newly emerging (at X-ray temperatures) bright points both inside CHB regions and CHs. They typically start with a brightening in just a few XRT pixels (4–6) somewhere in a pre-existing BP which we believe to be the reconnection site. Shimojo et al. (1996) reported from the statistical study of 100 jets in SXT/Yohkoh observations that most of them were associated with micro-flares in the foot-points of the jets. Shimojo et al. (2007) resolved the fine structure of a quiet Sun X-ray jet to be the expansion and eruption of loop structures colliding with the ambient magnetic field, similar to the CH jet. Madjarska (2010) studied in great detail one of the jet-like phenomena identified in the datasets analysed here. The author estimated that the reconnection site reaches temperatures of up to 12 MK from observations of Fe XXIII 263 Å from EIS/Hinode, which confirms that some of these events are very similar to large flares but on a much smaller spatial scale. Seconds after the reconnection takes place, a cloud of plasma is blown out from the BP. Madjarska (2010) reported that although the event appears more like a jet (although some expanding loops can also be distinguished) in X-ray images as observed in projection on the solar disk, the two additional view points from STEREO/SECCHI reveal that the phenomenon evolves as an expulsion of BP loops followed by a collimated flow along the quasi-open field lines of the expanded loops. The escaping plasma reaches temperatures of around 2 MK (Culhane et al. 2007; Madjarska 2010).

Nisticò et al. (2009) found 5 out of 79 jets analysed from STEREO/SECCHI observations exhibiting a three part structure typically of coronal mass ejections (CMEs) – bright leading edge, a dark void and bright trailing edge (e.g. the prominence material). The authors named them micro-CMEs. The rest were called Eiffel tower-type jets, where the reconnection appears to happen on top of the loops and lambda-type jets with reconnection occurring in the jet foot-points. As most of the events studied here were seen in projection on the solar disk, this visual division into different groups is not possible. However, the visual examination of the phenomena analysed here confirms that expulsion of BP loops describes these features best, hence, we will further refer to them as EBPLs (Eruptive BP loops).

Figure 5 presents an example of a typical EBPL event from a BP happening along an ECH boundary. The EBPL ends with the BP vanishing at X-ray temperatures triggering the coronal hole to expand. The plasma ejected from the BP seems to collide with structures on its way (propagating towards the QS region seen in projection on the solar disk) setting off a brightening in a pre-existing BP (denoted with B in Fig. 5) with no obvious plasma outflows.

We also found that the presence of a transient CH in the quiet Sun triggers the occurrence of EBPL-like phenomena, similar to the equatorial and polar CH ones. Yet again, the evolution of the BPs along the boundaries changed the CHBs (Fig. 6). Due to the smaller size of the TCH, these changes lead to a large expansion or contraction of the TCH, in some cases even a disappearance. In Fig. 7 we give a series of images which exhibit one of the quiet Sun events. In comparison to CHs, the events identified in the quiet Sun images rarely show outflows (Table 2). Neither

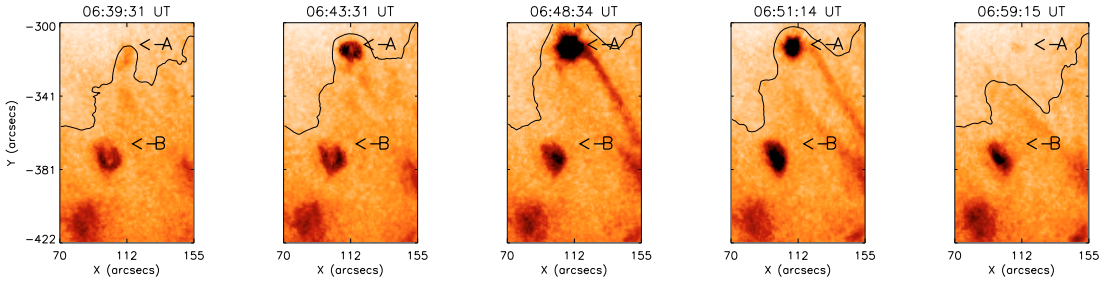

Fig. 5. An example of a typical jet-like happening on 2007 November 12 at the coronal hole boundaries. A refers to the jet while B refers to the BP.

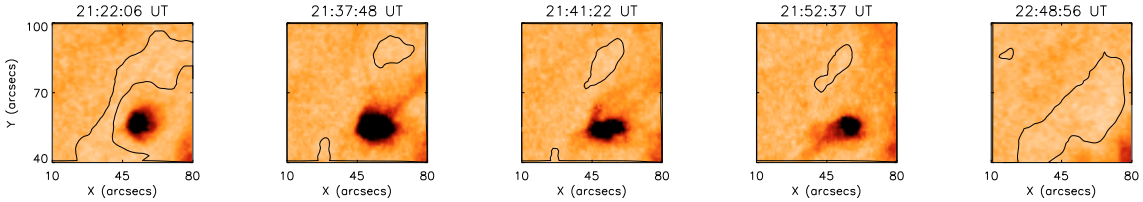

Fig. 6. A bright point which produced several jet-like events at the boundaries of a transient coronal hole on 2007 November 29.

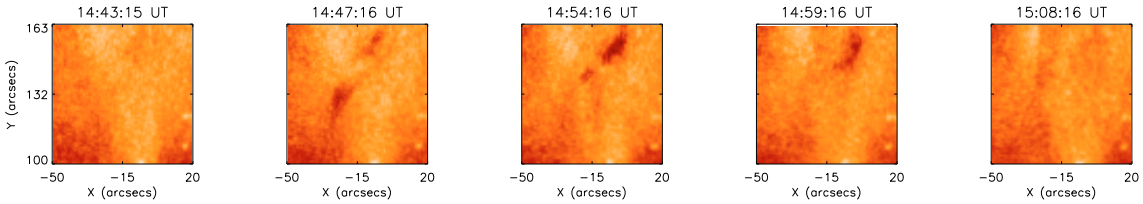

Fig. 7. An example of a brightening event identified in quiet Sun data obtained on 2009 January 10.

expanding loops nor collimated flows were distinguishable in the XRT images (i.e. no EBPL).

This brings us to the numerical comparison of CHBRs and CHs with QS areas. We find an average of 75 brightening events per 100×100 arcsec^2 per day for the coronal holes and boundaries and 20 events in the quiet Sun. Approximately 70% of these brightenings in CHs and CHBRs showed plasma outflows while only 30% of the brightenings seen in the quiet Sun exhibit jet-like structures. Previous works indicated fewer events per day either because of the poorer spatial resolution of the instrument used or because of the visual identification methods.

The identified brightening events with no plasma outflows could either be driven by two sided loop reconnection (Shibata et al. 1994) between emerging fluxes and overlying coronal fields, in which the ejected plasma flow along the closed loop structures, or reconnection driven brightenings with plasma outflows at much lower temperatures. They can also represent flows in loop structures, perhaps triggered by reconnection shocks from the neighbourhood as seen in the example brightening event B in Fig. 5. Shimojo et al. (2007) showed that a QS jet appears to be guided by the closed magnetic field lines (loops), unlike the jets in the CHs and CHBRs which are guided by the open magnetic field lines. This result immediately raises the question whether the presence of open magnetic field lines is crucial for the generation of outflow phenomena.

Comparison of the physical properties such as duration and size of the jet-like events in ECHs and polar CHs show no difference. A good correspondence was found between the duration and the size of the events, irrespective of their position. The larger events have longer duration of around 40 min and are mostly associated with pre-existing coronal bright points or at least with features becoming visible in X-rays just before the eruption. The smaller events have a shorter duration of around 20 min (mostly with no pre-existing features at coronal temperatures). However, for most events the actual duration from the moment the reconnection occurs (i.e. when the plasma is ejected) until the plasma outflow is no longer evident is usually between 10 and 15 min. The amount of plasma ejected entirely depends on the magnetic energy available before the reconnection and it will, therefore, differ from event to event. Repetitive occurrence of jets in the same bright points are more common in CHs than in the QS. No periodicity was found, although a large number of BPs produced several jet-like events (from 2 to 5 times) during the course of the observations until all the stored magnetic energy was exhausted and the bright point fully disappeared.

The proper motions of the outflows obtained from space-time plots are in the range of 100–500 km s^{-1} for most of the events. Because of the projection effect of the jets with respect to the solar disk, the velocity we obtain gives the lower boundary of the real velocity of the ejected plasma. Based on their plasma velocity we divide X-ray jets into two groups: (i) jets with pre-existing coronal structures (X-ray BPs) which have velocities $\approx$350 km s^{-1} or greater (i.e. in the range of the Alfvén velocity in the lower corona) and (ii) jets with no pre-existing structures at X-ray temperatures, showing velocities of around 150 km s^{-1} (i.e. close to the Alfvén velocity in the transition region). Stereo EUV images taken with the 171 Å filter confirm the presence of a corresponding reconnection jet-like structures at transition region temperatures.

5. Conclusions

The present article confirms our findings from Paper I that the evolution of loop structures known as coronal bright points is

associated with the small-scale changes of CHBs. We were able to identify the true nature of these changes which represent plasma outflows associated with the expansion of bright point loop structures. The plasma trapped in the loop structures is consequently released along the "quasi" open magnetic field lines. These ejections appear to be triggered by magnetic reconnection, most probably the so-called interchange reconnection (Wang & Sheeley 2004) between the closed magnetic field lines (BPs) and the open magnetic fields of coronal holes. The ejected plasma is guided and accelerated further away from the Sun by the open magnetic field lines with some jets reaching several solar radii (Nisticò et al. 2009). Contrary, in the quiet Sun the plasma ejected as a result of two or one sided loop reconnection, is contained in the corona by the closed magnetic field lines.

Tall and extended coronal loops are very rare in coronal holes (Wiegelmann & Solanki 2004), while closed (loop) magnetic structures of varying physical properties are ubiquitous in the quiet Sun corona as seen in EUV and X-ray observations. Coronal holes with predominant open magnetic fields and minority closed loop structures (BPs) are encompassed by these loop structures seen at transition region and coronal temperatures. Woo et al. (2004), Widing & Feldman (2001) and Feldman et al. (2005) showed that the elemental abundance of trapped plasma is proportional to the confinement time of the plasma in loop structures. Newly emerged active region loop structures were found to have initial photospheric abundances (FIP bias $\approx$1–2) which increased with time, reaching $\approx$5 in 1–3 days (Widing & Feldman 2001). Schrijver et al. (1998) concluded that $\approx$1.5 days is the reconfiguration time-scale for the supergranulation network magnetic fields where coronal BPs have their foot-points rooted. This time period is in the range of the confinement time-scale needed for the enhancement of the FIP bias.

Coronal BPs electron densities were derived from CDS onboard SoHO in the temperature range $1.3–2 \times 10^6$ K by Ugarte-Urra et al. (2005). The authors concluded that the bright points plasma have properties which are more similar to active region plasma rather than quiet Sun plasma, although BPs do not show the increase of electron density at temperature over LogT_e $\sim$ 6.2 K, observed in the core of active regions (Ugarte-Urra et al. 2005). These results were later confirmed from data taken with the Extreme-ultraviolet Imaging Spectrometer (EIS) for LogT_e $\sim$ 6.1 and 6.2 K (Pérez-Suárez et al. 2008). The BP lifetime in EUV were found to be on average 20 h in the EUV (Zhang et al. 2001) and on average 8 h in X-rays with some BPs lasting up to 40 h (Golub et al. 1974). The results of individually studied BPs by Ugarte-Urra et al. (2004) give for two BPs a lifetime of 38 and 51 h detected in Fe XII 195 Å images from Extreme-ultraviolet Imaging Telescope (EIT) on-board SoHO and by Pérez-Suarez (Ph.D. thesis 2009) in five BPs: BP1 – 48 h, BP2 more than 54 h, BP3 – 37 h, BP4 – 45.2 h and BP5 – 35 h (on the limb). The study by Golub et al. (1974) on BPs lifetime in X-rays has not been updated so far using Hinode X-ray observations. The BPs properties given above strongly suggest that their plasma can become enriched on low FIP elements.

Raouafi et al. (2008) concluded that X-ray jets are the precursors of polar plumes, and jets happening in pre-existing polar plumes enhance the brightness of the plume haze. Polar plumes are observed even at several solar radii (Deforest et al. 1997) and were found to contribute to the solar wind stream. They have been reported to occur even at low latitudes (Wang & Sheeley 1995). Jets, associated with BPs, were also recently registered with the Large Angle and Spectrometric Coronagraph on-board SoHO (Wang & Muglach 2008) and SECCHI/STEREO (Nisticò et al. 2009). Hence, the BP plasma cloud, which is ejected as a result of magnetic reconnection, will therefore, escape from the Sun having the plasma characteristics of the slow solar wind. We asked ourselves whether the plasma ejections we observe can possibly be a source of the fast solar wind? This possibility cannot be fully rejected, although it is a fact that these jets happen sporadically rather than continuously, which is in contradiction with the nature of the fast solar wind.

Our specially designed observing programs provided us with spectroscopic co-observations from SUMER, CDS and EIS along with the XRT and SOT. In a follow up paper we will derive the physical properties such as velocity, density, temperature and others of a large number of events happening in the FOV of the spectrometers.

Acknowledgements. The authors thank ISSI, Bern for the support of the team "Small-scale transient phenomena and their contribution to coronal heating". Research at Armagh Observatory is grant-aided by the N. Ireland Department of Culture, Arts and Leisure. We also thank STFC for support via grants ST/F001843/1 and PP/E002242/1. Hinode is a Japanese mission developed and launched by ISAS/JAXA, with NAOJ as domestic partner and NASA and STFC (UK) as international partners. It is operated by these agencies in co-operation with ESA and NSC (Norway). The STEREO/ SECCHI data used here are produced by an international consortium of the Naval Research Laboratory (USA), Lockheed Martin Solar and Astrophysics Lab (USA), NASA Goddard Space Flight Center (USA), Rutherford Appleton Laboratory (UK), University of Birmingham (UK), Max-Planck-Institut für Sonnensystemforschung (Germany), Centre Spatiale de Liège (Belgium), Institut d'Optique Théorique et Appliquée (France), and Institute Astrophysique Spatiale (France).

References

Ahmad, I. A., & Webb, D. F. 1978, Sol. Phys., 58, 323
Culhane, L., Harra, L. K., Baker, D., et al. 2007, PASJ, 59, 751
Deforest, C. E., Hoeksema, J. T., Gurman, J. B., et al. 1997, Sol. Phys., 175, 393
DeForest, C. E., Martens, P. C. H., & Wills-Davey, M. J. 2009, ApJ, 690, 1264
DeForest, C. E., Plunkett, S. P., & Andrews, M. D. 2001, ApJ, 546, 569
Doyle, J. G., Popescu, M. D., & Taroyan, Y. 2006, A&A, 446, 327
Feldman, U., Landi, E., & Schwadron, N. A. 2005, J. Geophys. Res. (Space Phys.), 110, 7109
Golub, L., Deluca, E., Austin, G., et al. 2007, Sol. Phys., 243, 63
Golub, L., Krieger, A. S., Silk, J. K., Timothy, A. F., & Vaiana, G. S. 1974, ApJ, 189, L93
Krieger, A. S., Timothy, A. F., & Roelof, E. C. 1973, Sol. Phys., 29, 505
Madjarska, M. S., & Wiegelmann, T. 2009, A&A, 503, 991
Madjarska, M. S., Doyle, J. G., & van Driel-Gesztelyi, L. 2004, ApJ, 603, L57
Moreno-Insertis, F., Galsgaard, K., & Ugarte-Urra, I. 2008, ApJ, 673, L211
Nisticò, G., Bothmer, V., Patsourakos, S., & Zimbardo, G. 2009, Sol. Phys., 120
Pérez-Suárez, D., Maclean, R. C., Doyle, J. G., & Madjarska, M. S. 2008, A&A, 492, 575
Raouafi, N.-E., Petrie, G. J. D., Norton, A. A., Henney, C. J., & Solanki, S. K. 2008, ApJ, 682, L137
Saito, K. 1965, PASJ, 17, 1
Savcheva, A., Cirtain, J., Deluca, E. E., et al. 2007, PASJ, 59, 771
Schrijver, C. J., Title, A. M., Harvey, K. L., et al. 1998, Nature, 394, 152
Shibata, K., Ishido, Y., Acton, L. W., et al. 1992, PASJ, 44, L173
Shibata, K., Nitta, N., Matsumoto, R., et al. 1994, in X-ray solar physics from Yohkoh, ed. Y. Uchida, T. Watanabe, K. Shibata, & H. S. Hudson, 29
Shimojo, M., Hashimoto, S., Shibata, K., et al. 1996, PASJ, 48, 123
Shimojo, M., Narukage, N., Kano, R., et al. 2007, PASJ, 59, 745
Ugarte-Urra, I., Doyle, J. G., & Del Zanna, G. 2005, A&A, 435, 1169
Ugarte-Urra, I., Doyle, J. G., Madjarska, M. S., & O'Shea, E. 2004, A&A, 418, 313
von Steiger, R. 1996, in Cool Stars, Stellar Systems, and the Sun, ed. R. Pallavicini, & A. K. Dupree, ASP Conf. Ser., 109, 491
Wang, Y.-M., & Sheeley, Jr., N. R. 1995, ApJ, 446, L51
Wang, Y.-M., & Sheeley, Jr., N. R. 2004, ApJ, 612, 1196
Wang, Y.-M., & Muglach, K. 2008, Sol. Phys., 249, 17
Wang, Y.-M., Sheeley, Jr., N. R., Walters, J. H., et al. 1998, ApJ, 498, L165
Widing, K. G., & Feldman, U. 2001, ApJ, 555, 426
Wiegelmann, T., & Solanki, S. K. 2004, Sol. Phys., 225, 227
Woo, R., Habbal, S. R., & Feldman, U. 2004, ApJ, 612, 1171
Zhang, J., Kundu, M. R., & White, S. M. 2001, Sol. Phys., 198, 347